Earthq Eng & Eng Vib (2020) 19: 725-737 **DOI**: https://doi.org/10.1007/s11803-020-0591-9

Vibration analysis of damaged and undamaged steel structure systems: cantilever column and frame

Muhammad Abuzar Khan[1†], Kareem Akhtar[1‡], Naveed Ahmad[2‡], Feroz Shah[1‡] and Naeem Khattak[1§]

1. *Department of Mechanical Engineering, University of Engineering & Technology, Peshawar KPK 25120, Pakistan*

2. *Earthquake Engineering Center, Department of Civil Engineering, UET Peshawar, Pakistan*

Abstract: This paper presents the experimental and numerical studies conducted on a steel column and a steel frame structure using free vibration analysis. The effects of damages on structures were investigated, which were simulated by introducing multiple cracks at different locations in the experimental and numerical models. The acceleration responses of the test models, were recorded through an accelerometer, and were used to calibrate the numerical models developed in finite element based software. Modal frequencies of damaged and undamaged structures were compared and analyzed, to derive relationships for damaged and undamaged structures' frequencies in terms of crack depth. It was found that, due to the presence of cracks, the mechanical properties of a structure changes, whereby, the modal frequencies decrease. An approximately linear trend was observed for the frequency decrease with the increase in crack depth, which was also confirmed by the numerical models. The derived relationships were extended to further develop a mechanics-based damage scale for steel structures, to help facilitate structural health monitoring and screening of vulnerable structures.

Keywords: frequencies degradation; steel structures; damage scale; structural health monitoring; free vibrations

1 Introduction

Columns, beams and frames are widely used as structural components for carrying compression and bending loads, respectively, in a majority of mechanical and civil structures and infrastructures. Beams and columns are connected together to form frames for carrying vertical loads due to gravity, and lateral loads due to wind and earthquake actions. Steel structures provide resistance to the external applied loads through the development of internal normal and shear stresses in the structural members, and through the development of shear and bearing stresses at the connections, e.g. bolted members. The design and safety of such structural members are generally based on the initial uncracked section properties. The damage present in any structural member causes changes in the physical parameters and mechanical properties of a structure, e.g., cross-sectional area, moment of inertia, flexure and shear rigidity, which dictate the health of the structure, and which are essential for identifying maintenance requirements. The early identification of structural damage is vital to avoid structural failure in case of extreme loading conditions, which undetected can result in catastrophic conditions. Presently, there is a lack of simple methods and procedures that can facilitate prompt assessment of structural health and quickly screen structures for such risk. In the present study, vibration analysis was carried out, both experimentally and numerically, to study the effect of pre-existing structural damages on the fundamental vibrations of structures, and further, to derive simple analytical formulae for correlating structural damage with vibration characteristics of structures, which can be essential for structural health monitoring.

1.1 Literature review

In recent years, significant work has been done in the field of structural health monitoring, with the aim to evaluate the health of structures for identification of any required maintenance or repair. Recent researchers (Behzad *et al*., 2005; Kshirsagar and Bhuyar, 2010; Mia *et al*., 2017) have discovered through numerical analyses of cantilever beams that natural frequencies are reduced due to the presence of cracks. It was also found that the amount of decrease largely depends on the area and the size of the crack. It was found that the frequencies are less affected by the presence of cracks at a distance from the secured end, i.e., fixed boundary condition, where the bending moment and sectional curvature demands

Correspondence to: Muhammad Abuzar Khan, Department of Mechanical Engineering, University of Engineering & Technology, Peshawar KPK 25120, Pakistan
Tel: +92-3339829091
E-mail: abuxarkhan01@gmail.com, naveed.ahmad@uetpeshawar.edu.pk
[†]Engineer; [‡]Assistant Professor; [§]Professor
Received November 21, 2018; **Accepted** May 27, 2019

are relatively less. Similar observations have been made by Jagdale and Chakrabarti (2013) such that, for a particular crack location, the natural frequencies are inversely proportional to crack depth, and the reduction in frequencies is higher where the bending moment is more vigorous. In earlier research (Ostachowicz and Krawczuk, 1991), based on the numerical analysis of beams, it was found that the reduction in frequency becomes most immense in cases where the cracks in members are adjacent to each other. Similarly, analysis of columns has demonstrated a difference in modular properties and mundane frequencies of the damaged and undamaged cases (Khan *et al*., 2014). Khalate and Bhagwat (2016) and Owolabi *et al*. (2003), carrying out an experimental study on the analysis of a beam, engendering multiple cracks in the beam, and giving precise locations and depths of crack, observed a great reduction in the natural frequencies of cracks near the restrained end. Ramanamurthy and Chandrasekaran (2011), by performing finite element analysis for a composite cantilever beam, concluded that the damage was identified by increasing values of crack depth and damage severity. Penny *et al*. (1993) predicted that any method of damage location is critically dependent on the accuracy of the damage model, and further, that it is difficult to calculate frequencies at higher modes. Neves *et al*. (2016) has observed that the stiffness of a cracked beam is less than the stiffness of an un-cracked beam, and that condition was reflected in the decrease of the natural frequencies of the cracked beam and in its free dynamic response. Luo *et al.* (2005) focused on studying the dynamic behavior of cracked structures by using the finite element approach (FEA), summarizing that the crack surface is persistently in an open state, i.e., the opposing sides of the crack do not come into contact during vibration. Anifantis and Dimarogonas (1983) discovered that the existence of cracks in columns can significantly affect the stability of the vertically loaded columns. Altunışık *et al*. (2017), conducted modal parameter identification and vibration-based damage detection by using the finite element method and experimental measurements of multiple cracked cantilever beams with hollow circular sections. They discovered that cracks strongly affect the natural frequencies of the beam; at the cracked section the frequencies decreased non-monotonically in response to the reduction in flexural stiffness of the beam at the damaged section. Chinka *et al*. (2018) observed that modal analysis is used easily to observe the effect of cracks on the natural frequencies and mode shapes for a range of crack locations and crack depth. Altunışık *et al*. (2018) analyzed vibrations of a multiple damaged cantilever beam with box-section by transfer matrix method, finite element method, and operation modal analysis. Gaviria and Montejo (2016) obtained results for structural health monitoring showing that the system's dynamic parameters can be used to determine the occurrence of damage, and that robust estimation of the stiffness matrix can be used to size and locate the damage. Tao *et al*. (2014) developed a method that can be used to sense and localize damage-induced nonlinearities in structures under seismic excitation. The nonlinearity behavior of the structure, such as opening and closing of the cracks in concrete and yielding of steel, can be noticed in the real structure.

Antunes *et al*. (2012) used the optical technology sensor to verify the practicality of tall dynamic structures. Their work showed that it is possible to get the Eigenfrequencies, which can be used to calculate the reaction of structures along a lifetime. Ikemoto *et al*. (2014) found that damage evaluation of a frame structure is possible when a change in the natural frequency and maximum strain ratio is observed for a structure. Baruh and Ratan (1993) identified the position of damage by establishing a damage detection system. The detection is done in two parts. First, the Eigensolution is identified using a modal identification technique. Then, the identified Eigensolution is used together with the properties of the eigenvalue problem to sense the damage components. Kharrazi *et al*. (2002) recognized damage by using the finite element model, updated with the experimental study of different damage cases. Hearn and Testa (1991) concluded that the position of a crack in the structure is determined using changes in natural frequency derived from the equation of motion. Damage to a structure is seen to influence natural frequencies and mode shapes. Foti (2013) proposed two methods for damage identification in bridges using simulated data for a simply supported structure. The change in Mode Shapes method and Mode Shapes Curvature methods is not properly sensitive to damage since the change in displacement mode shapes is generally too small. Wahab and Roeck (1999) showed that the modal curves of the lower modes are more precise than those of higher ones. They concluded that attention should be given when using the modal curves of higher modes for damage recognition.

Kim *et al*. (2003) conducted an experimental study on a simply supported steel truss bridge. He identified the mode shapes of the bridge with high precision and accuracy. They observed that the change in modal frequencies and mode shapes for the damaged cases cause high-stress distribution and global stiffness loss. Zhou *et al*. (2010) added that vibration-based monitoring techniques (VBMT) have proved useful for the detection and localization of structural damages. Yan *et al*. (2007) found that frequency change can detect the presence of structural damage, while determining the location of structural damage requires information of the vibration mode. Kessler *et al*. (2002) investigated a potential role of the frequency response of a composite structure in an SHM system by validating the numerical and experimental model. Good agreement was found between numerical and experimental results for lower frequencies, but the comparison was impractical for the modes at higher frequencies.

Demir and Özener (2019) assessed the capability

of numerical simulation by comparing the acceleration time histories and displacements with the measured counterparts. There results gathered information that the seismic shear stresses did not reduced due to the existence of the column in the ground. Godínez-Domínguez and Tena-Colunga (2019) observed the chief elements responsible for dissipating the earthquake input energy, yielding mappings for different load-steps were achieved using both nonlinear static and dynamic analyses. Furthermore, dynamic parameters for the response maxima were acquired from the story and global hysteresis plots. Rahman *et al*. (2019) validated the simulation model for the wind turbine tower with an experimental study in terms of natural frequency, mode shape and uncontrolled response at the 1st mode. Fakhraddini *et al*. (2019) performed the nonlinear dynamic analyses on Eccentrically Braced Frames. The results have been post-processed by nonlinear regression analysis in order to identify the key parameters that effect the peak displacement pattern of these frames. Results display that proposed displacement patterns have comparatively good agreement with those developed by an exact nonlinear dynamic analysis.

Tang *et al*. (2019) established a finite element model to determine the critical structural components. Then, the engineering requirements and the framework of the monitoring system are studied based on the results of numerical analysis. The specific implementation of the structural health monitoring is then carried out, which comprises of sensor selection, installation and wiring. Hu *et al*. (2019) performed finite element analysis of the cantilever beam. The optimal sensor placement for the best response reconstruction is determined by the projected method based on the updated FE model of the beam. Next the sensors are mounted on the physical cantilever beam, a number of experiments are performed. The responses at key locations are reconstructed and compared with the measured ones.

Although previous studies confirm that natural frequency decreases due to the presence of a crack, they do not provide a relationship between crack depth and frequency decrease. Also, multiple cracks were engendered for the column structures and multiple cracks were studied simultaneously. Previous studies are mostly carried out on beams and are numerical-calculation based. In this study, the free vibration analysis of undamaged and damaged (cracked) column and frame structures are performed using both experimental and numerical calculations. Natural frequencies are extracted from the damaged and undamaged column and frame structures both numerically and experimentally and then compared to show the rigor of damage affecting the health of the structure. The comparison between the numerical and experimental study is presented, and the results provide a good agreement of both cases.

2 Experimental study

Experiments were performed on column and frame structures separately. The column consisted of a squared cross-section, and the material of the column was steel. The dimensions of the column were 1000 mm length and a cross-sectional area of 12.5 mm. The frame model was a single-story steel structure. Three squared beams were welded together to form a frame structure. The dimensions of the beams were 1000 mm of length and a cross-sectional area of 31 mm.

In order to find the mechanical properties of the materials, standard tensile tests were conducted for column and frame specimens. Dog bone samples were created for both structures according to ASTM standard specification. The mechanical properties of column and frame structures are tabulated in Table 1 and Table 2.

The column was instrumented with a single accelerometer. The accelerometer was screwed to the top end of the column structure as shown in Fig. 1. The frame structure was instrumented with an accelerometer. The accelerometer was screwed to the top end of the structure where the two beams were joined by a welded joint as shown in Fig. 7. Accelerometer (model # 1703469, Dytran /accuracy of 492.2 mv/g) converted the vibrational signal into a voltage signal that was further analyzed by the data acquisition systems to show the response of the structure. Free vibration analysis of undamaged structures were recorded by striking them with the face of the hammer. The structures were induced to vibrate, and the accelerometers recorded the data. This data from the accelerometer was subjected to the data acquisition system which filtered the data

Table 1 Mechanical properties/ dimensions for column strucutre

Properties/ dimensions	Yield stress	Length, l	Width, w	Depth, d	Young′s modulus	Density	Poison ratio
Values	279.32 N/mm^2	1000 mm	12.5 mm	12.5 mm	200 GPa	0.128 kg/m^3	0.30

Table 2 Mechanical properties/ dimensions for frame sructure

Properties/ dimension	Length, l	Width, w	Depth, d	Young′s modulus	Density	Poison ratio	Yield stress
Values	1000 mm	31 mm	31 mm	200 GPa	7700 kg/m^3	0.30	377.437 N/mm^2

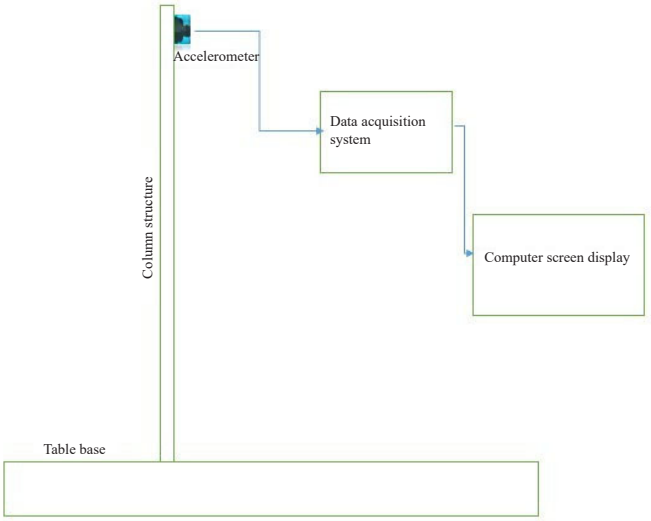

Fig. 1 Block diagram of column structure

Fig. 2 Zoom view of undamaged and structure damaged column for experimentation

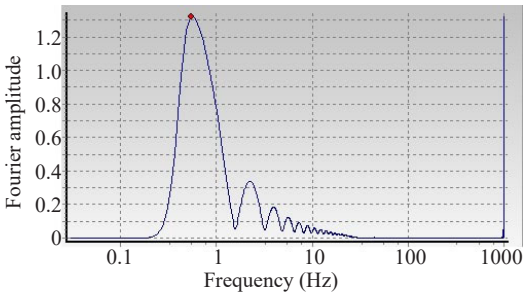

Fig. 3 Undamaged column response

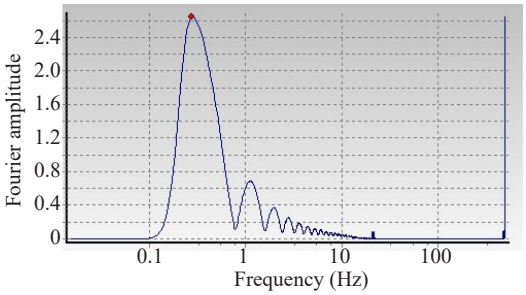

Fig. 4 3 mm damaged column response

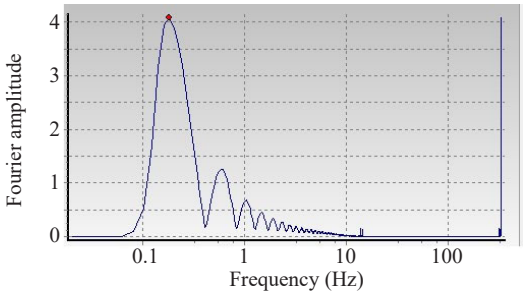

Fig. 5 6 mm damaged column response

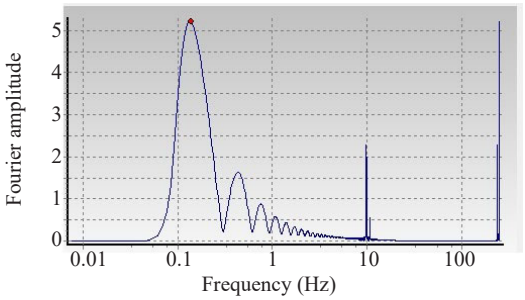

Fig. 6 8 mm damaged column response

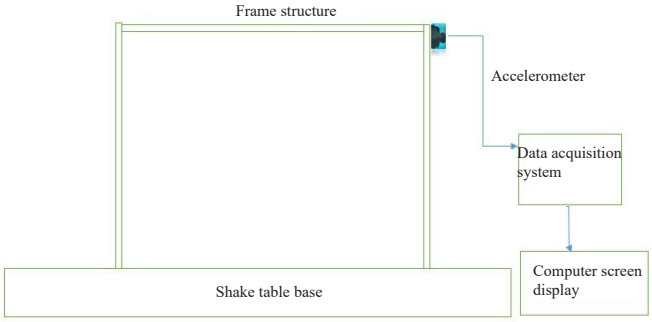

Fig. 7 Block diagram of frame structure

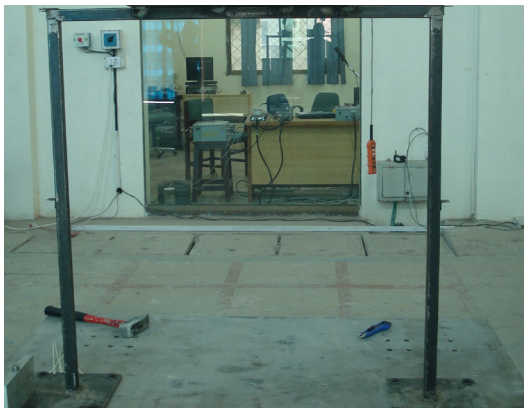

Fig. 8 Undamaged frame structure

and removed unwanted noise signals. The output of the data acquisition system was a text file. This text file was analyzed in the software SeismoSignal, which provided the modal frequencies of the mechanical structures. The natural frequencies for the column and frame structures were obtained from the plots depicted in Figs. 3 to 6

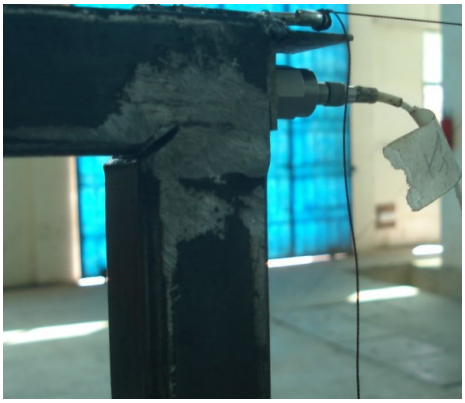

Fig. 9 Zoom view of damaged structure 10 mm crack

Fig. 10 Zoom view of damaged structure 20 mm crack

Fig. 11 Zoom view of damaged structure 30 mm crack

Fig. 12 Zoom view of accelerometer attached to the top end

and Figs. 13 to 16. The crests in the plots correspond to the natural frequencies and were extracted using the frequency at the peaks of the plots. We were interested in measuring the global lateral response of the structure; therefore, the installation of a single accelerometer at the top of the structure was enough to provide the global acceleration response of the model. The numerical to experimental comparison also considered the same reference for global response simulations.

The acceleration response measured by the accelerometer at the top included the global response for all the modes. The present study included signal processing and fast Fourier transform (FFT) for transforming the time-domain signal to frequency domain. The latter provided clear information in terms of the energy and frequency contents of the signal; e.g., the FFT plot exhibits spikes at the dominating frequencies, where the amplitude and width of spike indicate the amount of energy for each frequency. In the present study the modal frequencies identified through FFT were compared with the numerically calculated frequencies for fundamental and higher modes. SeismoSignal software was used. In this module, the fourier amplitude spectrum and the power spectrum (or power spectral density function) were computed by means of fast Fourier transformation (FFT) of the input time-history. The Fourier amplitude spectrum shows how the amplitude of the ground motion is distributed with respect to frequency, effectively meaning that the frequency content of the given accelerogram can be fully determined. The power spectral density function, on the other hand, may be used to estimate the statistical properties of the input ground motion and to compute stochastic response using random vibration techniques.

The column and frame structures were damaged to extract the natural frequencies of the cracked structures. The column was damaged at three different depths, i.e., 3 mm, 6 mm and 8 mm at a distance of 250 mm from the fixed end. Vibration Analysis was performed for each crack depth. Then the column was damaged further at the center with three different depths, i.e., 3 mm, 6 mm and 8mm.Vibration analysis was again performed for each case. The frame structure was damaged at three different depths, i.e., 10 mm, 20 mm, and 30 mm at the joint of the structure. Figures 7–12 show the experimental setup of the frame structure.

3 Analytical solution

The stiffness, time-period and frequency of the column structures were determined by the following equations.

$$K = 12\frac{EI}{l^3}$$

The modulus of elasticity (E) was calculated from

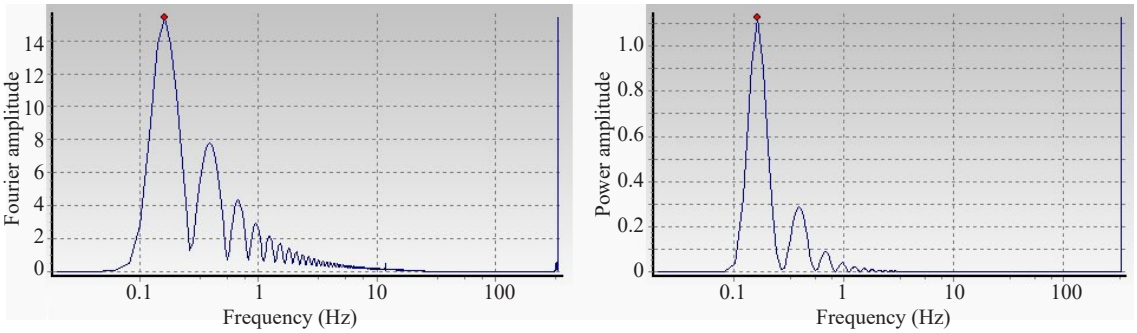

Fig. 13 Undamaged frame response

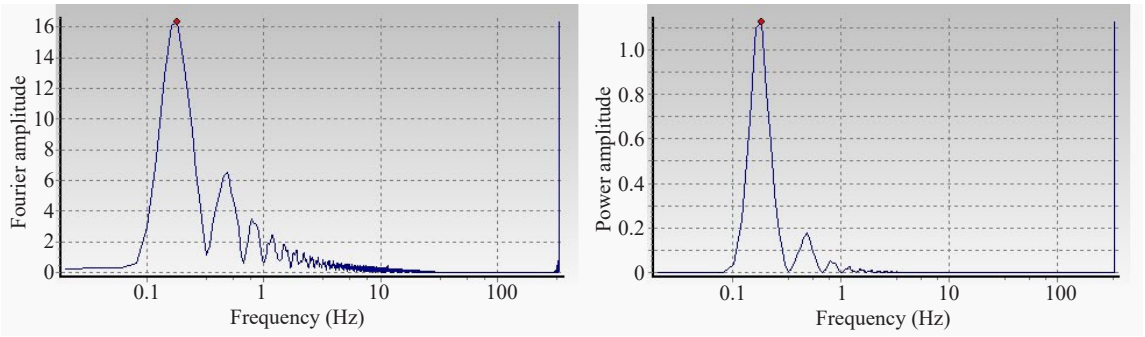

Fig. 14 10 mm damaged frame response

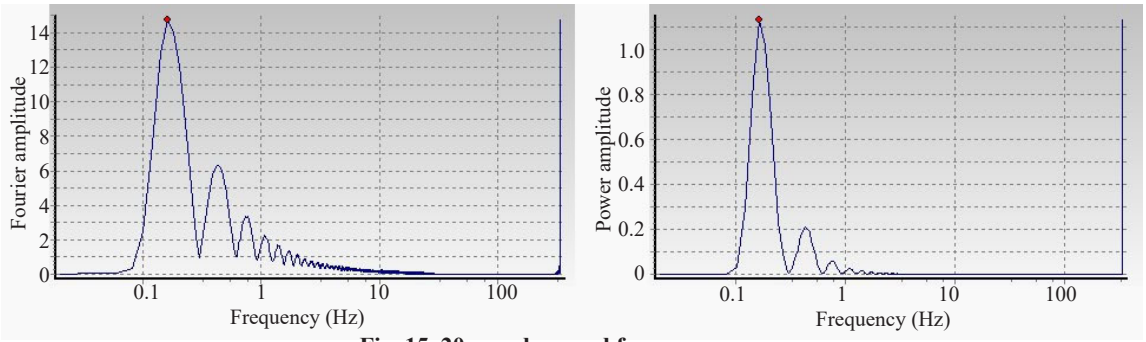

Fig. 15 20 mm damaged frame response

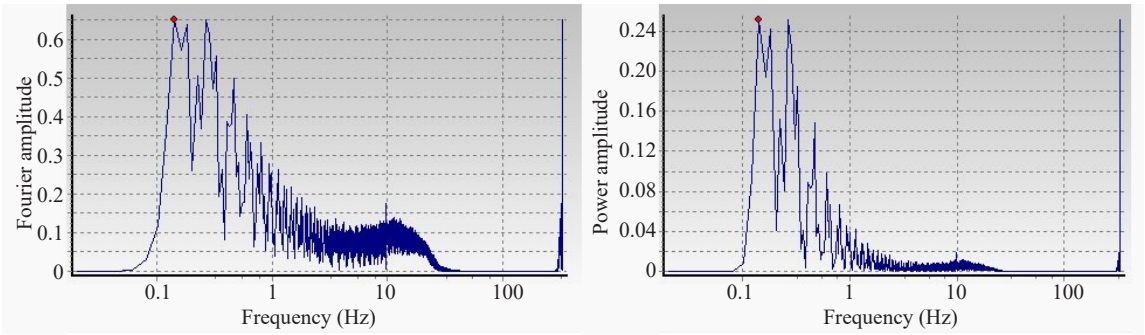

Fig. 16 30 mm damaged frame response

the tensile test and found to be 200 GPa. The moment of inertia of the column (I), and length (l) of the column was 1 m.

$$T = 2\pi\sqrt{\frac{M}{K}}$$

The mass of the column was determined from a digital scale

$$f = \frac{1}{2\pi\sqrt{\frac{M}{K}}}$$

Putting the values in the above equation gave us the frequency of the structures.

4 Numerical analysis

The column and frame structures were modeled in the ABAQUS 6.14 software for finite element analysis. The dimensions and the mechanical properties of the column and frame structures are illustrated in Table 1 and Table 2. Boundary conditions were imposed at the bottom of the column to make it a fine-tuned column and at the bottom of the frame structure to make it a fixed steel structure. The first three modal frequencies of the structures were extracted for free vibration analysis.

All the dimensions and crack locations for column and frame structures in numerical model were kept exactly the same as in experimental models. Cracks were created by deleting finite regions in the numerical model, which is a common approach for creating damages.

Figure 17 shows the undamaged and damaged column structure for different crack depths. Figures 18–21 depicts the undamaged and damaged frame structure for different crack depths.

(a) Undamaged column (b) 3 mm damaged (c) 6 mm damaged (d) 8 mm damaged column

Fig. 17 Undamaged and damaged column with different crack depths in simulation software

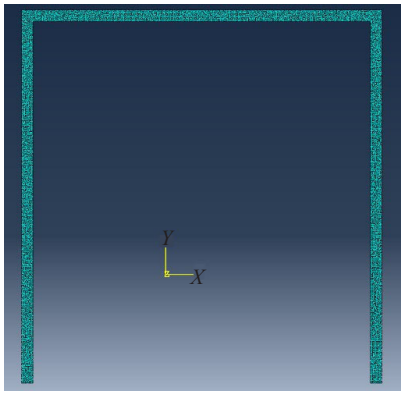

Fig. 18 Undamaged structure

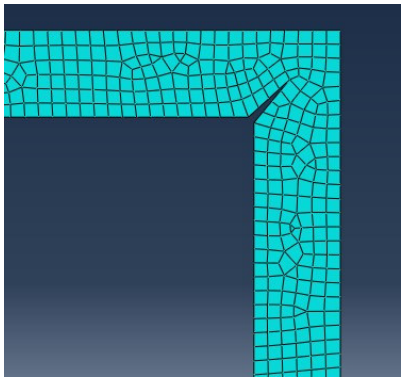

Fig. 20 Damaged structure 20 mm crack

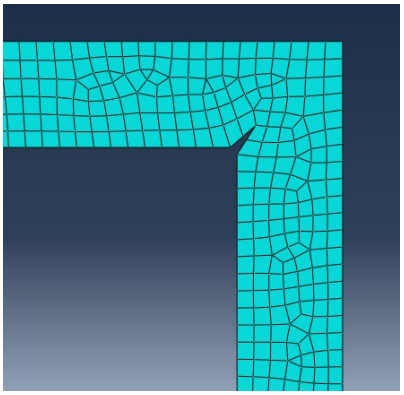

Fig. 19 Damaged structure 10 mm crack

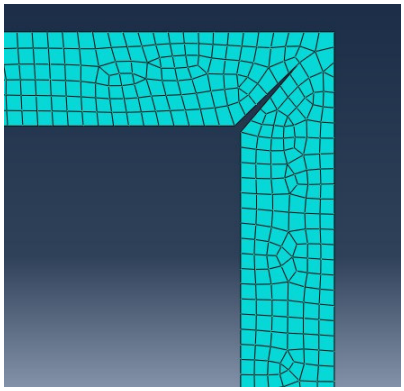

Fig. 21 Damaged structure 30 mm crack

5 Mesh convergence study

Mesh for column structure was generated using ABAQUS. Four different meshes, i.e., coarse, medium, fine and very fine, were generated to study mesh independence. The details of the mesh size are given in Table 3. The natural frequencies of the column structure were calculated using linear perturbation method in the finite element software. As shown in Table 3, there is negligible difference in the natural frequencies values, indicating that our first mesh is suitable for analysis, which is also time efficient. Hence, all the results reported here were produced using coarse mesh as tabulated in Table 3.

6 Results and discussion

The numerical and experimental data was recorded for undamaged and damaged mechanical structures. First, the column was damaged near the fixed end; after that, the column was damaged again at the center of the column to create multiple cracks. The frame structure was damaged at a single location at the joint where beams were welded together. The crack was induced in the column at the length of 250 mm from the restrained end, with crack depths of 3 mm, 6 mm, and 8 mm. Two dimensionless parameters were defined as crack depth ratio and frequency ratio. Crack depth ratio is the ratio of the depth of crack to the width of the structure. The frequency ratio is the ratio of damaged frequency to the undamaged frequency for the first three modes of vibrations. The frequency ratios for the experimental and numerical cases were plotted against the crack depth ratios when the crack was modeled near the fixed end of the column.

The plots for the first mode as seen in Fig. 22 show a linear decrease in the frequency ratio when the crack depth ratio increases, i.e., when the crack depth increases. The graphs for numerical and experimental cases show a little variation among each other when the crack depth increases. In the second and third mode, as depicted in Figs. 23 and 24, when the frequency ratios are plotted for the numerical and experimental cases against the crack depth ratios, the frequency ratio can be seen to follow the same linearly decreasing trend as the damage level in the column increases. The pattern of the graph is the same as it is for the first mode. The outcome for both experimental and numerical simulation is within the limits of agreeable error. The frequency ratio for the first three modes shows a slight decrease in the frequency ratios for the depth of 3 mm to 6 mm, while for the crack depth at 8 mm the frequency ratios decrease

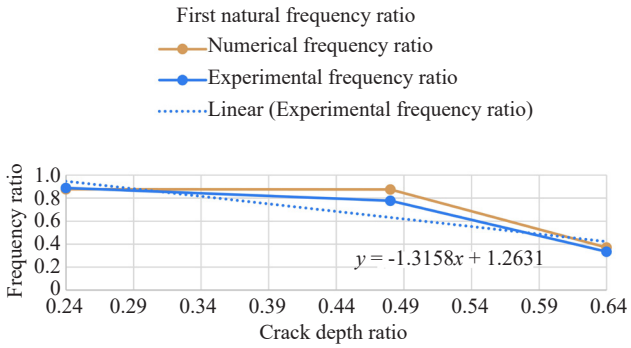

Fig. 22 Numerical and experimental comparison for the first mode of vibration for a crack near the fixed end

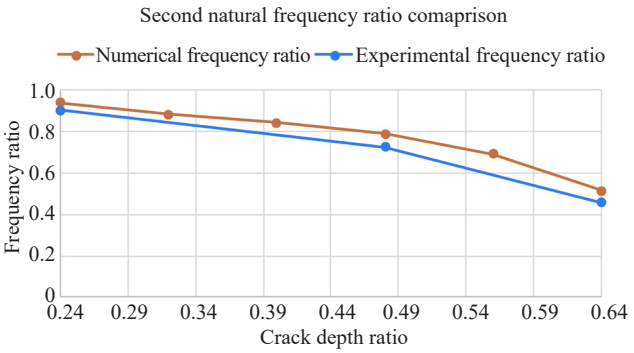

Fig. 23 Numerical and experimental comparison for the second mode of vibration for a crack near the fixed end

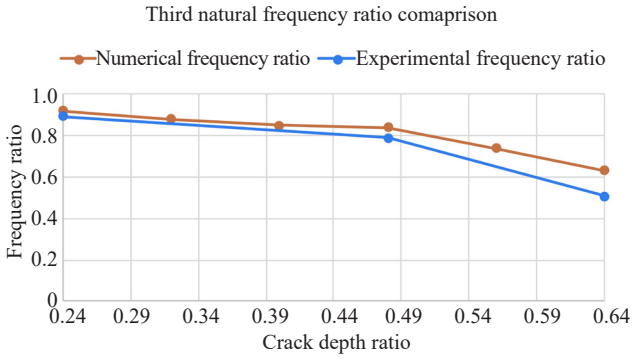

Fig. 24 Numerical and experimental comparison for the third mode of vibration for a crack near the fixed end

Table 3 Mesh properties for column structure

Mesh type	Number of elements	First natural frequency	Second natural frequency	Third natural frequency
Coarse mesh	1425	0.0659033	0.26713	0.41921
Medium mesh	2688	0.065733	0.26613	0.41911
Fine mesh	4098	0.064912	0.26331	0.41903
Very fine mesh	9879	0.064386	0.26299	0.40123

rapidly, which indicates that the structure is going to failure. When the numerical and experimental results are plotted together, we see that there is less variation in the frequency ratio for both numerical and experimental cases. The data show a promising result for the first three modes when the crack is modeled near the restrained end (250 mm). The comparison of both numerical and experimental cases justifies the results of both cases.

The comparison was drawn showing the plots for both numerical and experimental cases. The comparison of the frequency ratio for the numerical and experimental cases is tabulated in Table 4.

7 Experimental and numerical results for multiple cracks

For multiple cracks, the column was damaged at a second location, 500 mm from the fixed end. The crack near the fixed end depth was constant, i.e., 8 mm, however, three depth cases were taken into the account. The crack depth of 3 mm, 6 mm, and 8 mm were modeled at the center of the column. First three natural frequencies for each depth case were calculated both experimentally and numerically. The first natural frequency ratio for the different crack depth ratios is depicted in Fig. 25. The plot follows a linearly decreasing trend. The results show that when the crack is positioned away from the fixed end, the frequencies tend to decrease as the damage level in the column increases. However, the frequency does not decrease as drastically as it does for the crack positioned near the fixed end. The numerical and experimental frequency ratios were plotted for the second and third mode where the crack is positioned at the center of the column, as shown in Figs. 26 and 27. The outcome from the results shows a linear decrease in the frequency ratios when the crack depth ratio is increased. The data from both numerical and experimental cases show a little variation among each other, and both plots show a linearly decreasing trend. The frequency ratios are not severely affected by the crack when it is modeled at the center of the column, whereas the frequency ratios decreased drastically when the crack was modeled near the fixed end. The numerical

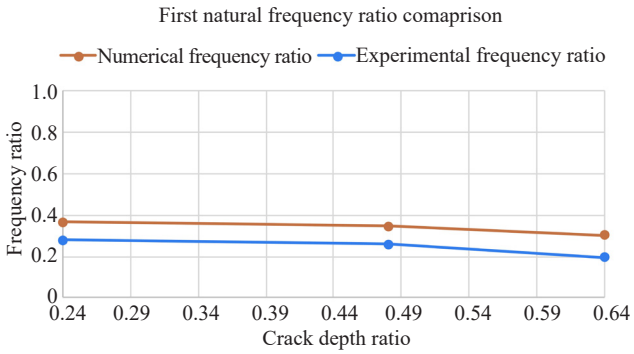

Fig. 25 Numerical and experimental comparison of the first mode for the crack positioned away from the fixed end

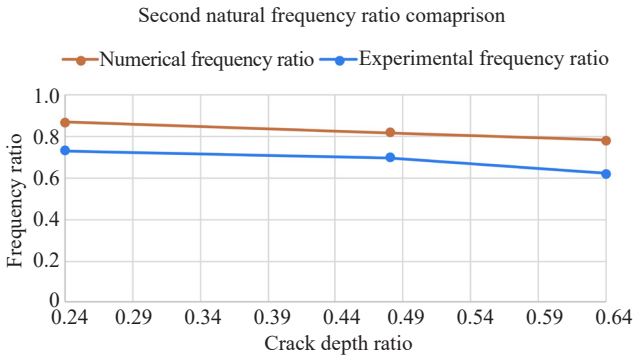

Fig. 26 Numerical and experimental comparison of the second mode for the crack positioned away from the fixed end

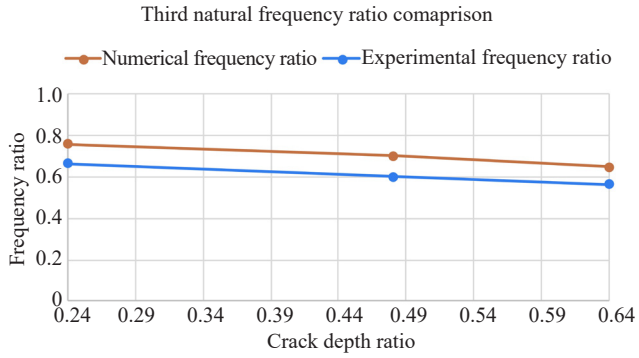

Fig. 27 Numerical and experimental comparison of the third mode for the crack positioned away from the fixed end

Table 4 Numerical and experimental comparison for the first three modes of vibration for a crack near the fixed end

	Crack depth ratio	Numerical frequency ratio	Experimental frequency ratio	Age error (%) Frequency to numerical difference
First natural frequency ratio	0.24	0.87805	0.88888	1.2
	0.48	0.85723	0.77776	-9.2
	0.64	0.30761	0.33333	8.3
Second natural frequency ratio	0.24	0.93934	0.90549	-3.6
	0.48	0.78861	0.72506	-8.05
	0.64	0.51371	0.45638	-11.15
Third natural frequency ratio	0.24	0.92143	0.89406	-2.9
	0.48	0.83971	0.78812	-6.14
	0.64	0.63311	0.50605	-20

and experimental comparison for each damage scenario and three modal frequencies are tabulated in Table 5.

For both experimental and numerical cases, it is noticeable that when the crack is induced into the column the modal frequencies are affected. As well, it can be optically discerned that the frequency ratios decrement as the crack depth in the column structure increments. Moreover, the reduction in frequencies is greatly affected by the crack being present near the fixed end. If we keep incrementing crack depth near the fine-tuned end, a time will come when the failure of the structure will transpire. Additionally, from the above data, it can also be described that crack depth away from the fine-tuned end does not readily affect the health of the column. Moreover, there is a linear decrease in the frequency ratios when the crack depth keeps incrementing.

8 Frame structure

The comparison was drawn for the numerical and experimental cases for the frame structure. The results were plotted together to show the response of the structure for the three depth cases, as discussed earlier. There is a linear decrease in the frequency ratio for increasing damage level. Thus, from these comparisons, it is pragmatic that the frequencies are in mutual correspondence with each other. The comparison of numerical and experimental data for the first, second and third mode shows a linearly decreasing trend for different crack depth ratios, as depicted in Figs. 28–30. The plots illustrate that the numerical and experimental data show less variation in the frequency ratios. The error in the data is miniscule, and it is observed that the frequency ratios for both cases are in mutual correspondence with each other.

The numerical and experimental comparison for each damage scenario of a frame structure and three modal frequencies are tabulated in Table 6.

It can be visually perceived from the comparison of the numerical and experimental results that the frequency ratio is reduced when the crack in the structure advances. The results for the numerical and experimental cases are

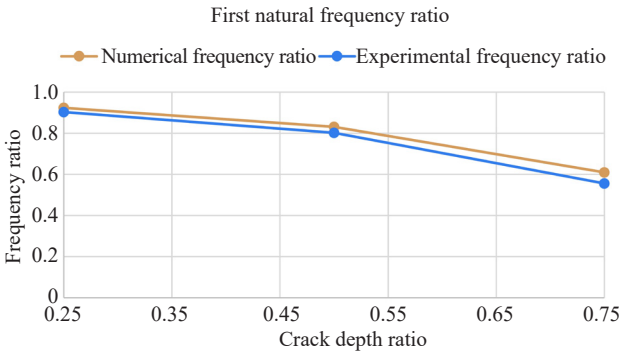

Fig. 28 Numerical and experimental comparison for the first mode of vibration

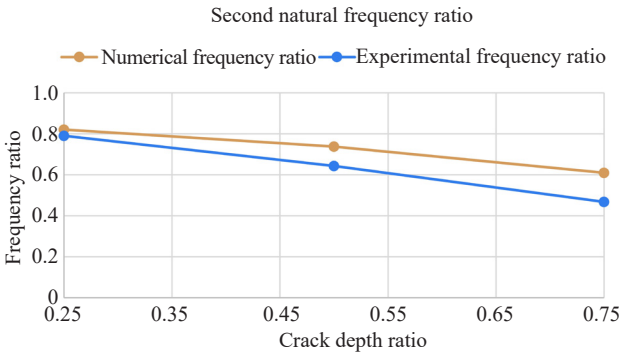

Fig. 29 Numerical and experimental comparison for the second mode of vibration

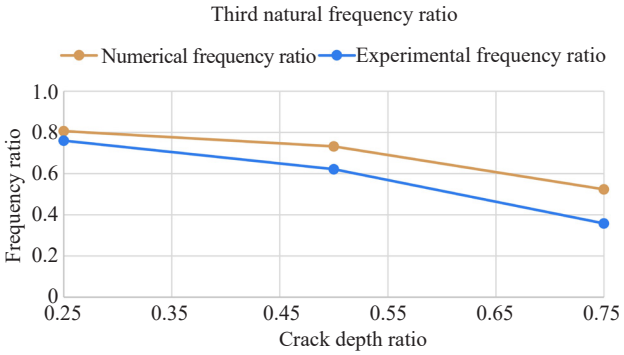

Fig. 30 Numerical and experimental comparison for the third mode of vibration

Table 5 Numerical and experimental comparison for the first three modes of vibration for a crack at the center of the column

	Crack depth ratio	Numerical frequency ratio	Experimental frequency ratio	Age error (%)
First natural frequency ratio	0.24	0.36853	0.27866	-24.3
	0.48	0.34553	0.25988	-24.7
	0.64	0.30138	0.19437	-35
Second natural frequency ratio	0.24	0.86925	0.73325	-15.6
	0.48	0.82158	0.70021	-14.7
	0.64	0.78339	0.66211	-15.4
Third natural frequency ratio	0.24	0.75951	0.66711	-12.1
	0.48	0.70078	0.60037	-14.3
	0.64	0.64861	0.56429	-13

in less error. We can say that the data of both cases is promising and comparable.

9 Development of damage scale for steel members

We realize that cracking in structural members occurs primarily under imposed loads due to gravity, e.g., superimposed dead loads and live loads due to people and contents, and lateral loads, e.g., due to winds and earthquakes. Further, considering an elastic-perfectly plastic inelastic behavior of structural steel members, the frequency of a member, which has been damaged under the application of loads, decreases in relation with the member displacement ductility demand, as follows;

$$\mu = \frac{1}{\left(\frac{f_{\mathrm{d}}}{f_{\mathrm{ud}}}\right)^2}$$

where μ is the displacement ductility demand, measured as the ratio of inelastic displacement demand to the yield displacement capacity of the member, f_{d} is the frequency of the damaged member (cracked member), while f_{ud} is the frequency of the counterpart undamaged member. The above relationship can be used to calculate the member displacement ductility demand on a member for a specified decrease in the member frequency, or alternatively, to calculate the decrease in member frequency given the displacement ductility demand. The experimental and numerical data with regard to the frequency decrease in steel columns, for the engendered cracks in the column, was analyzed to correlate the frequency decrease to the crack depth. A relationship was established between the ratios of damaged-to-undamaged frequency of column to the crack depth ratio x, using constraint regression analysis:

$$\left(\frac{f_{\mathrm{d}}}{f_{\mathrm{ud}}}\right) = 1 - 0.75x$$

where f_{d} is the frequency of damaged column, f_{ud} is the frequency of counterpart undamaged column, and x is the ratio of crack depth to the total depth of column. Furthermore, knowing the curvature demand on a cantilever structural member, the yield displacement capacity of the member can be formulated, as follows:

$$\Delta_{\mathrm{y}} = \frac{1}{3}\phi_{\mathrm{y}} h^2$$

where Δ_{y} is the yield displacement capacity, ϕ_{y} is the yield curvature capacity of the section, and h is the height of the column. The above equation can be also extended to beam members, considering double bending condition and equal moments at the end restraints, replacing the factor 1/3 by 1/6. Interestingly, inelastic analysis of steel sections has shown that the yield curvature of a steel section can be related to the section depth and steel yield strain capacity:

$$\phi_{\mathrm{y}} = \frac{2\varepsilon_{\mathrm{y}}}{d}$$

where d is the section depth, and ε_{y} is the yield strain capacity of steel material. The above equations for yield displacement and yield curvature capacities can be used in conjunction with the $f_{\mathrm{d}}/f_{\mathrm{ud}}$ relationship to derive a formula for calculating inelastic displacement demand on the column under lateral loads, in terms of member chord rotation:

$$\theta = \frac{2}{3}\left(\frac{h\varepsilon_{\mathrm{y}}}{d}\right)\frac{1}{(1-0.75x)^2}$$

where θ is the member chord rotation. For a cantilever column under later load, it is quantified as the ratio of the displacement demand of free end to the height of the column. This parameter can be used for member damage assessment and verification of structures. For example, considering a more practice case of G60 steel, with yield strength of 60 ksi (415 MPa), cantilever column of height

Table 6 Numerical and experimental comparison for the first three modes of vibration for frame structure

	Crack depth ratio	Numerical frequency ratio	Experimental frequency ratio	Age error (%)
First natural frequency ratio	0.25	0.92309	0.90278	2.2
	0.50	0.83095	0.80247	-3.4
	0.75	0.61007	0.55561	-8.9
Second natural frequency ratio	0.25	0.82014	0.78976	-3.7
	0.50	0.73804	0.64329	-12.8
	0.75	0.61007	0.46785	-23
Third natural frequency ratio	0.25	0.80597	0.75961	-5.7
	0.50	0.73248	0.62090	-15
	0.75	0.52402	0.37581	-28

3 m, and depth 300 mm. Assuming that a crack has been formed in the column under lateral load, with crack depth ratio $x = 0.20$, which is 20% of the column depth. Using the basic hooks law will provide yield strain ε_y of 0.0021. Furthermore, using the aforementioned equation will provide an estimate of curvature ϕ_y of 0.0138 (1/m), yield displacement Δ_y of 41.38 mm, and member chord rotation of 0.019 (1.90%). This means that any lateral load developing a crack in the column, at the critical section of 20% depth, will cause the column to undergo a member chord rotation of 1.90%. Increasing the crack depth up to 50% ($x = 0.50$), the member chord rotation will increase to 0.0353 (3.53%). It is worth mentioning that most codes allow only 2%– 2.5% of column chord rotation for seismic actions, in order to control inter-story drift under lateral imposed load and to protect the building partition walls. The derived equations can be used to identify the threshold crack depth, and similarly, can be used for screening of buildings vulnerable to seismic forces.

10 Conclusions

Experimental and numerical study of a column and frame structure, subjected to free vibration, was presented. Free vibration investigation was conducted to extract the natural frequencies of the structure. The column was damaged at three crack depths and at two different locations to discover the reaction of the column subjected to free vibration. The frame structure was damaged at three different crack depths at a joint to discover the reaction of the structure presented to free vibration. The plots show a linear relationship when the frequency ratio is plotted against the crack depth for various damaged scenarios for both structures. It is concluded that the modal frequencies of the structure decrease as the cracks in the structure increment near the restrained end of the column structure, and the frequencies also decrease when damage appears in the frame structure. For different crack depths, the decrease in modal frequencies is less as the crack moves away from the fine-tuned end. From the trends of the plots, it can be noticed that the trend of these ratios shows a linear response for both experimental and numerical cases. The data in both cases show a change in the modal frequencies when the crack appears in the structure. When the crack depth increases there is a decrease in the frequencies, and the decrease can be noted by considering the plots of the frequency ratio with respect to the crack depth. The crack in the structure does not propagate, and it is assumed that the free vibration does not affect the crack propagation in the frame structure. From the outcomes of this research it is established that when we keep increasing the crack depth near the fine-tuned end, the stiffness of the material decreases and the material becomes degraded. When we keep incrementing the crack depth in the structure, a time will come when the column structure will go to failure. With the decrease in natural frequencies and change in mode shapes, we can monitor the health of the column structure for various damage scenarios subjected to free vibration, to take safety precautions at the right time before the structure undergoes permanent failure.

Acknowledgment

The authors are thankful to the reviewers for the constructive remarks that helped in the improvement of the paper. The authors would relish expressing their gratitude to the Earthquake Engineering Center of University of Engineering & Technology Peshawar, for facilitating the authors in lab experiments and providing resources for the completion of the research work presented herein.

References

Altunışık AC, Okur FY and Kahya V (2017), "Modal Parameter Identification and Vibration Based Damage Detection of a Multiple Cracked Cantilever Beam," *Engineering Failure Analysis*, **79**: 154–170.

Altunışık AC, Okur FY and Kahya V (2018), "Vibrations of a Box-Sectional Cantilever Timoshenko Beam with Multiple Cracks," *International Journal of Steel Structures*.

Anifantis N and Dimarogonas A (1983), "Stability of Columns with a Single Crack Subjected to Follower and Vertical Loads," *International Journal of Solids and Structures*, **19**(4): 281–291.

Antunes P, Travanca R, Rodrigues H, Melo J, Jara J, Varum H and Andre P (2012), "Dynamic Structural Health Monitoring of Slender Structures Using Optical Sensors," *Sensors*, **12**(5): 6629–6644.

Baruh H and Ratan S (1993), "Damage Detection in Flexible Structures," *Journal of Sound and Vibration*, **166**(1): 21–30.

Behzad M, Meghdari A and Ebrahimi A (2005), "A New Approach for Vibration Analysis of a Cracked Beam," *International Journal of Engineering-Materials And Energy Research Center*, **18**(4): 319.

Chinka SB, Adavi B, and Putti SR (2018), "Influence of Crack on Modal Parameters of Cantilever Beam Using Experimental Modal Analysis," *Journal of Modeling and Simulation of Materials*, **1**(1): 16–23.

Demir S and Özener P (2019), "Numerical Investigation of Seismic Performance of High Modulus Columns Under Earthquake Loading," *Earthquake Engineering and Engineering Vibration*, **18**(4): 811–822. https://doi.org/10.1007/s11803-019-0537-2.

Fakhraddini A, Saffari H and Fadaee MJ (2019), "Peak Displacement Patterns for the Performance-Based Seismic Design of Steel Eccentrically Braced Frames," *Earthquake Engineering and Engineering Vibration*, **18**(2): 379–393. https://doi.org/10.1007/s11803-019-

0510-0.

Foti D (2013), "Dynamic Identification Techniques to Numerically Detect the Structural Damage," *The Open Construction and Building Technology Journal*, **7**(1): 43–50.

Gaviria CA and Montejo LA (2016), "Output-Only Identification of the Modal and Physical Properties of Structures Using Free Vibration Response," *Earthquake Engineering and Engineering Vibration*, **15**(3): 575–589.

Godínez-Domínguez EA and Tena-Colunga A (2019), "Behavior of Ductile Steel X-Braced RC Frames in Seismic Zones," *Earthquake Engineering and Engineering Vibration*, **18**(4): 845–869. https://doi.org/10.1007/s11803-019-0539-0.

Hearn G and Testa RB (1991), "Modal Analysis for Damage Detection in Structures," *Journal of structural engineering*, **117**(10): 3042–3063.

Hu RP, Xu YL and Zhan S (2018), "Multi-Type Sensor Placement and Response Reconstruction for Building Structures: Experimental Investigations," *Earthquake Engineering and Engineering Vibration*, **17**(1): 29–46. https://doi.org/10.1007/s11803-018-0423-3.

Ikemoto T, Yoshikawaii D, Yamashitaiii M, Miyajimaiv M and Kitaura M (2014), "A Study on Health Monitoring of Structural Damages for Two Stories Model by Using Vibration Test," *13th World Conference on Earthquake Engineering Vancouver*, B.C., Canada.

Jagdale PM and Chakrabarti MA (2013), "Free Vibration Analysis of Cracked Beam," *Int. J. Eng. Res. Appl*, **3**: 1172–1176.

Kessler SS, Spearing SM, Attalla MJ, Cenik CS and Soutis S (2002), "Damage Detection in Composite Materials Using Frequency Response Methods," *Composites Part B: Engineering*, **33**(1): 87–95.

Khalate AB and Bhagwat VB (2016), "Detection of Cracks Present in Composite Cantilever Beam by Vibration Analysis Technique," *IJISET-International Journal of Innovative Science, Engineering & Technology*, **3**(1): 400–404.

Khan IA, Yadao A and Parhi DR (2014), "Fault Diagnosis of Cracked Cantilever Composite Beam by Vibration Measurement and RBFNN," *Journal of Mechanical Design*, **1**(1): 1–4.

Kharrazi MH, Ventura CE, Brincker R and Dascotte E (2002), "A Study on Damage Detection Using Output-Only Modal Data," *Proceeding of the 20th International Modal Analysis Conference*.

Kim JT, Ryu YS, Cho HM and Stubbs N (2003), "Damage Identification in Beam-Type Structures: Frequency-Based Method vs. Mode-Shape-Based Method," *Engineering structures*, **25**(1): 57–67.

Kshirsagar SV and Bhuyar LB (2010), "Signature Analysis of Cracked Cantilever Beam," *International Journal of Advanced Research in Engineering and Technology*, **1**:105–117.

Luo TL, Wu JSS and Hung PJ (2005), "A Study of Non-Linear Vibrational Behavior of Cracked Structures by the Finite Element Method," *Journal of Marine Science and Technology*, **13**(3): 176–183.

Mia MS, Islam MS and Ghosh U (2017), "Modal Analysis of Cracked Cantilever Beam by Finite Element Simulation," *Procedia Engineering*, **194**: 509–516.

Neves AC, Simões FMF and DeCosta AP (2016), "Vibrations of Cracked Beams: Discrete Mass and Stiffness Models," *Computers & Structures*, **168**: 68–77.

Ostachowicz W and Krawczuk M (1991), "Analysis of the Effect of Cracks on the Natural Frequencies of a Cantilever Beam," *Journal of Sound and Vibration*, **150**(2): 191–201.

Owolabi GM, Swamidas AJS and Seshadri R (2003), "Crack Detection in Beams Using Changes in Frequencies and Amplitudes of Frequency Response Functions," *Journal of Sound and Vibration*, **265**(1): 1–22.

Penny J, D Wilson, *et al*. (1993), "Damage location in structures using vibration data," *Proceedings-SPIE*, The International Society for Optical Engineering.

Rahman M, Ong ZC, Chong WT and Julai S (2019), "Smart Semi-Active PID-ACO Control Strategy for Tower Vibration Reduction in Wind Turbines with MR Damper," *Earthquake Engineering and Engineering Vibration*, **18**(4): 887–902. https://doi.org/10.1007/s11803-019-0541-6.

Ramanamurthy E and Chandrasekaran K (2011), "Vibration Analysis on a Composite Beam to Identify Damage and Damage Severity Using Finite Element Method," *International Journal of Engineering Science and Technology* (*IJEST*).

Tang T, Yang DH, Wang L, Zhang JR and Yi TH (2019), "Design and Application of Structural Health Monitoring System in Long-Span Cable-Membrane Structure," *Earthquake Engineering and Engineering Vibration*, **18**(2): 461–474. https://doi.org/10.1007/s11803-019-0484-y.

Tao D, Mao C, Zhang D and Li H (2014), "Experimental Validation of a Signal-Based Approach for Structural Earthquake Damage Detection Using Fractal Dimension of Time Frequency Feature," *Earthquake Engineering and Engineering Vibration*, **13**(4): 671–680.

Wahab MA and De Roeck G (1999), "Damage Detection in Bridges Using Modal Curvatures: Application to a Real Damage Scenario," *Journal of Sound and Vibration*, **226**(2): 217–235.

Yan Y, Cheng L, Wu ZY and Yum LH (2007), "Development in Vibration-Based Structural Damage Detection Technique," *Mechanical Systems and Signal Processing*, **21**(5): 2198–2211.

Zhou G, Wang DW, Li F, Zhang L, Li N, Wu ZS, Wen L, Lu GQ and Cheng HM (2010), "Graphene-Wrapped Fe3O4 Anode Material with Improved Reversible Capacity and Cyclic Stability for Lithium ion Batteries," *Chemistry of Materials*, **22**(18): 5306–5313.